In situ probing of helium desorption from individual nanobubbles under electron irradiation

M.-L. David,[a] F. Pailloux, V. Mauchamp, and L. Pizzagalli
Institut Pprime, UPR 3346 CNRS-Université de Poitiers-ENSMA, SP2MI, 86962 Futuroscope-Chasseneuil cedex, France

(Received 15 March 2011; accepted 4 April 2011; published online 26 April 2011)

The understanding of the mechanisms of helium bubble formation and evolution in materials requires the quantitative determination of several key quantities such as the helium density in the bubbles. Helium nanobubbles of about 16 nm in diameter were created in silicon by helium implantation at high fluence and subsequent annealing. Individual nanobubbles were analyzed by spatially resolved Electron Energy-loss Spectroscopy (EELS). We report on the *in situ* probing of helium desorption from the nanobubbles under electron irradiation. This opens new perspectives for a more accurate determination of the helium density through spatially resolved EELS. © *2011 American Institute of Physics*. [doi:10.1063/1.3582612]

In many materials, He introduced in high concentration may aggregate with vacancies, leading to the formation of bubbles which can modify the electrical and mechanical properties of the materials. The formation of bubbles is a long standing problem for structural materials used in nuclear reactors, He bubbles being responsible for the embrittlement of the materials.[1] This has triggered a very recent interest on interfaces in composite materials that can act as sinks for radiation-induced defects.[2–4] On the contrary, in the framework of defect engineering, He is introduced on purpose in semiconductors to create bubbles that could find many technological applications: annihilation of dislocations in GaN,[5] reducing the threading dislocation density via the enhancement of the strain relaxation of SiGe/Si heterostructures,[6] proximity gettering of metallic impurities[7] or recently, fabrication of ultrathin buried oxide layers in silicon.[8] On a more fundamental point of view, rare gas bubbles are interesting embedded nanosystems to study plasmon excitations,[9] or nanofluidics, as the nanobubbles can be an alternative route to previous study,[10] to create nanoholes. In this context, the understanding of nanobubble formation and evolution mechanisms, including the release of He, is of crucial importance.

In Si, bubbles of about 2 nm in diameter are created by He implantation at high fluence.[11] During subsequent annealing, the average size of the bubbles increases by either an Ostwald ripening process or by motion and coalescence, release of He occurs and ultimately bubbles evolve into voids. The release of He during annealing has been investigated by thermal desorption spectroscopy,[12–14] the activation energy being independent on the implantation conditions.[13] Less well known is a possible desorption due to irradiation. Recently, using gas phase ionization mass spectrometry, He reemission has been shown to occur also during implantation,[15] highlighting the key role of irradiation. These techniques are however not spatially resolved and the He release from an individual nanobubble during implantation/irradiation or during annealing is not accessible. In metals and alloys, spatially resolved Electron Energy-Loss Spectroscopy (EELS) experiments have been shown to be a powerful tool to determine He density in individual nanobubbles, through the measurement of the He $1s \rightarrow 2p$ transition integrated intensity.[16–19] Another approach, based on the determination of the blue shift of the He K-edge as compared to its position for the free atom [21.218 eV (Ref. 20)] could in principle provide an easier way to determine the He density in nanobubbles. This shift

$$\Delta E = C \times n_{\mathrm{He}}, \tag{1}$$

where n_{He} is the He density, is attributed to the short range Pauli repulsion between electrons of neighboring atoms. The constant of proportionality, C, has been determined theoretically, and experimentally for He bubbles in metals, see Refs. 17–19 and references inside. However, discrepancies are reported in the literature, C ranging from 0.016 to 0.044 $\mathrm{eV.nm^3}$. This prevents an accurate determination of the He density using the easier blue shift method.

The aim of this letter is twofold. First, we report on the *in situ* probing of He desorption from individual nanobubbles embedded in silicon under electron irradiation. Second, we show that these experiments can be used to determine C with a high accuracy, opening thus new perspectives for the determination of the He density in bubbles through the blue shift of the He K-edge.

Helium bubbles were created by He implantation in n-type (001) silicon samples using the following conditions: fluence of 7×10^{16} $\mathrm{cm^{-2}}$, energy of 50 keV, current of 10 μA and room temperature (RT). The samples were then submitted to annealing at 700 °C during 30 min under vacuum in a tubular furnace. These implantation and annealing conditions lead to the formation of a layer of bubbles of about 5 to 20 nm in diameter. Cross sectional transmission electron microscopy (TEM) samples were prepared by mechanical polishing down to 10 μm and ion milling in a GATAN-PIPS apparatus at low energy (2.5 keV Ar) and low incidence ($\pm 8°$) to minimize irradiation damage. The TEM samples were mounted in a cooling sample holder, operated at −176 °C. *In situ* electron irradiation and spatially resolved EELS experiments were performed using a JEOL 2200 FS microscope (Schottky-FEG, 200 kV, energy resolution of 0.7 eV) fitted with an omega filter. Spectrum images of 128 spectra of 2048 px were acquired using the following condi-

[a]Electronic mail: marie-laure.david@univ-poitiers.fr.

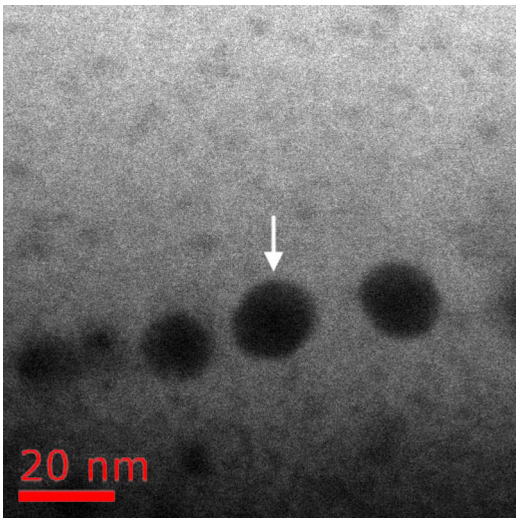

FIG. 1. (Color online) HAADF image of bubbles created by a 7×10^{16} cm^{-2}, 50 keV, RT, He implantation in (001) n-silicon followed by an annealing at 700 °C during 30 min. The bubble marked by an arrow has been analyzed in more details.

tions: probe size of 0.2 nm, acquisition time of 200 ms per spectrum with step increments of ranging from 0.2 to 0.6 nm, energy dispersion of 0.0675 eV/channel. The current in the probe was 10 pA.

Spatially resolved EELS experiments were performed on bubbles of 14 to 18 nm in diameter, see Fig. 1. The raw data were first realigned on the elastic peak and submitted to a multivariate statistic analysis[21] to remove the statistical noise. A typical low-loss spectrum recorded in the center of a bubble (the bubble marked by an arrow in Fig. 1) is depicted on Fig. 2. As seen, the He K-edge is clearly resolved at about 23 eV. The He density was determined using[16,17]

$$n_{\mathrm{He}} = \frac{I_{\mathrm{He}}}{I_{\mathrm{ZL}}} \frac{1}{\sigma_{\mathrm{He}} h}, \tag{2}$$

where I_{ZL} and I_{He} are the integrated intensities of the elastic peak and the He K-edge (over 3 eV) respectively, σ_{He} is the

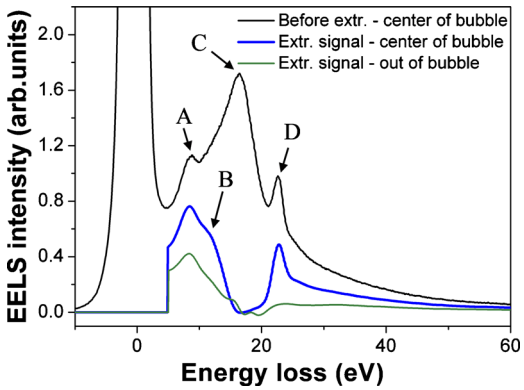

FIG. 2. (Color online) EEL spectra extracted from the spectrum image recorded on a 16 nm in diameter He bubble (marked by an arrow in Fig. 1). Top spectrum (black): raw data realigned on the elastic peak and analyzed via MSA, this spectrum is taken in the middle of the bubble. Middle spectrum (blue): extracted spectrum using our procedure (deconvolution of multiple scattering and Si plasmon fitting), taken in the same region than the black spectrum. Bottom spectrum (green): extracted spectrum taken in a region out of the bubble, to show the background signal. A is attributed to the SiO_2/Si interface plasmon (Refs. 22 and 23), B is the cavity plasmon (Ref. 24), C the silicon plasmon, and D is the He K-edge.

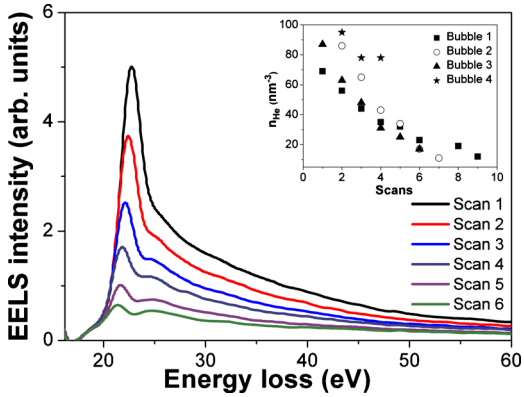

FIG. 3. (Color online) EEL spectra successively measured on the same bubble (all taken from the same region of the bubble marked by an arrow in Fig. 1). In the inset, estimated He density [through Eq. (2)] as a function of the successive measurements for four different bubbles.

angle-integrated cross-section for the $1s \rightarrow 2p$ excitation evaluated for the experimental conditions and h is the cavity thickness crossed by the electron beam. h was estimated as the complement to the local thickness measurements of the matrix as suggested in Ref. 18. The He K-edge was extracted from the EELS spectra using the following procedure: the multiple scattering was deconvoluted using a Fourier-log method and the Si plasmon was fitted using a sum of Lorentzian and Gaussian functions. A typical extracted spectrum is shown in Fig. 2. This figure also shows an extracted spectrum taken from a region out of the bubble to highlight the background signal. As seen, this signal is very low in the He K-edge region, that validates our extraction procedure. The signal to noise and to background ratio is thus very good, highlighting the benefit to work on Si: the He K-edge is not to close to the Si plasmon, allowing for a good quality signal extraction. As at least 50 spectra were acquired within a bubble during each scan, the mean He density and mean He K-edge energy shift were calculated by averaging the 15 to 20 data points acquired in the highest bubble thickness region to minimize surface effects.[18] The mean He density is estimated to be 86 ± 11 He/nm^3 for this bubble.

Successive spatially resolved EELS scans were performed on the very same bubble. Typical extracted EEL spectra are plotted in Fig. 3. As seen, the He K-edge exhibits a redshift and its intensity decreases, suggesting that the He density is decreasing at each scan. This is confirmed by the inset of Fig. 3, where the mean He density is plotted as a function of the number of scans for four bubbles. As seen, the mean He density is estimated to be about 90 He/nm^3 at the first scan and it decreases to a bit less than 20 He/nm^3 after six to nine scans. This clearly shows that electron irradiation induces He detrapping from the bubbles at a rate of about 25% per scan. It is worth noticing that this phenomenon is not operative at RT. Moreover, we have not observed any decrease of the estimated He density measured in the highest bubble thickness regions (15 to 20 EEL spectra acquisitions) during any of the scans. This suggests that the physical phenomenon involved in the He desorption from the bubbles is probably linked to a long time scale relaxation phenomenon occurring between the scans.

This behavior can now be used to make an accurate determination of the proportionality constant C [Eq. (1)]. The He K-edge shift is plotted in Fig. 4 as a function of the mean

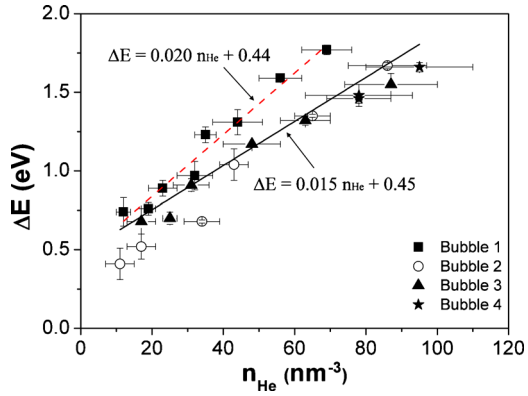

FIG. 4. (Color online) Shift in the He K-edge as compared to its position in atomic He as a function of the estimated He density. Full line (black): linear fit of the whole data set (all bubbles). Dashed line (red): linear fit of data points recorded for Bubble 1.

He density for successive scans performed on four bubbles. Our results confirm the linear relation between these two parameters. We have determined a value of C of 0.015 ± 0.005 eV.nm^3. The uncertainty corresponds to the highest difference between the value of C deduced from a linear fit of all data points and the value of C obtained for one bubble. As seen, the *in situ* observation of He desorption under electron irradiation allows for a very accurate determination of C as compared to previous studies. In these studies, C was indeed derived from measurements of the He density [using Eq. (2)] on several bubbles of different diameters (the He density is expected to be dependent on the bubble diameter). In this case, the highest source of uncertainties is certainly the evaluation of the bubble thickness crossed by the electron beam which is done either from the high angle annular dark field (HAADF) contrast[19] or from the complement to the Si thickness crossed by the electron beam.[18] In our study, the He density is determined on the very same bubble. Assuming no drift during the experiments, the bubble thickness crossed by the electron beam is thus always the same, seriously reducing the uncertainties.

In conclusion, we have shown that spatially resolved EELS experiments is a powerful tool to fully characterize He bubbles in Si in a similar way than that proposed in metals. We have clearly evidenced the He desorption from individual nanobubbles under electron irradiation by spatially resolved EELS. Finally, we have used these experiments to measure with a high accuracy the proportionality constant, C. Application of this approach to other materials opens new perspectives for the understanding of the formation and evolution mechanisms of He nanobubbles.

We are deeply indebted to Dr. Mathieu Kociak for fruitful discussions. We gratefully acknowledge Marc Marteau for performing the implantations.

[1]H. Trinkaus and B. N. Singh, J. Nucl. Mater. **323**, 229 (2003).
[2]N. Li, J. Carter, A. Misra, L. Shao, H. Wang, and X. Zhang, Philos. Mag. Lett. **91**, 18 (2011).
[3]M. Demkowicz, D. Bhattacharyya, I. Usov, Y. Wang, M. Nastasi, and A. Misra, Appl. Phys. Lett. **97**, 161903 (2010).
[4]N. Li, E. Fu, H. Wang, J. Carter, L. Shao, S. Maloy, A. Misra, and X. Zhang, J. Nucl. Mater. **389**, 233 (2009).
[5]D. Alquier, C. Bongiorno, F. Roccaforte, and V. Raineri, Appl. Phys. Lett. **86**, 211911 (2005).
[6]B. Hollander, S. Lenk, S. Mantl, H. Trinkaus, D. Kirch, M. Luysberg, T. Hakbarth, H. Herzog, and P. Fichtner, Nucl. Instrum. Methods Phys. Res. B **175**, 357 (2001).
[7]G. Petersen, S. Myers, and D. Follstaedt, Nucl. Instrum. Methods Phys. Res. B **127–128**, 301 (1997).
[8]X. Ou, R. Kögler, A. Mücklich, W. Skorupa, W. Möller, X. Wang, and L. Vines, Appl. Phys. Lett. **94**, 011903 (2009).
[9]R. Dhaka and S. Barman, Phys. Rev. Lett. **104**, 036803 (2010).
[10]A. Del Maestro, M. Boninsegni, and I. Affleck, Phys. Rev. Lett. **106**, 105303 (2011).
[11]V. Raineri, M. Saggio, and E. Rimini, J. Mater. Res. **15**, 1449 (2000).
[12]S. Godey, E. Ntsoenzok, T. Sauvage, A. van Veen, F. Labohm, M. Beaufort, and J. Barbot, Mater. Sci. Eng., B **73**, 54 (2000).
[13]E. Oliviero, M. David, M. Beaufort, J. Barbot, and A. van Veen, Appl. Phys. Lett. **81**, 4201 (2002).
[14]C. Griffioen, J. Evans, P. de Jong, and A. van Veen, Nucl. Instrum. Methods Phys. Res. B **27**, 417 (1987).
[15]K. Wittmaack, Appl. Phys. Lett. **92**, 051907 (2008).
[16]A. McGibbon, Inst. Phys. Conf. Ser. **119**, 109 (1962).
[17]C. Walsh, J. Yuan, and L. Brown, Philos. Mag. A **80**, 1507 (2000).
[18]D. Taverna, M. Kociak, O. Stéphan, A. Fabre, E. Finot, B. Décamps, and C. Colliex, Phys. Rev. Lett. **100**, 035301 (2008).
[19]S. Fréchard, M. Walls, M. Kociak, J. Chevalier, J. Henry, and D. Gorse, J. Nucl. Mater. **393**, 102 (2009).
[20]H. G. Kuhn, *Atomic Spectra* (Academic, New York, 1969).
[21]N. Bonnet, J. Microsc. **190**, 2 (1998).
[22]P. Moreau, N. Brun, C. Walsh, C. Colliex, and A. Howie, Phys. Rev. B **56**, 6774 (1997).
[23]T. Yamazaki, Y. Kotaka, and Y. Kataoka, Ultramicroscopy **111**, 303 (2011).
[24]M. Natta, Solid State Commun. **7**, 823 (1969).